FINAL TECHNICAL REPORT

to

NATIONAL AERONAUTICS AND SPACE ADMINISTRATION

From

California Institute of Technology
Division of Geological and Planetary Sciences
Pasadena, CA 91125

"Spacecraft Studies of Phobos and Mars"

(NAGW-1426)

Principal Investigator: Dr. Bruce C. Murray

Time Period: 6/1/88 - 10/31/90

Dr. Bruce C. Murray
Professor, Planetary Science
Division of Geological and
Planetary Science
California Institute of Technology
Pasadena, California 91125
(818) 356-3780

FINAL TECHNICAL REPORT
GRANT: NAGW-1426
P.I.: Bruce Murray

Attached, please find summaries of the major work done under this grant. They are taken from *Betts and Murray* [1993a], *Betts and Murray* [1993b], and *Betts, et al.* (abstract) [1990a].

The following publications and abstracts were produced at least in part from NAGW-1426:

Publications

Betts, B. H. and B. C. Murray, Thermally Distinct Ejecta Blankets from Martian Craters, *J. Geophys. Res.-Planets*, 98, 11,043-11,059, 1993a.

Betts, B. H. and B. C. Murray, Topical studies of the martian surface using the Termoskan data set, *J. Geophys. Res.-Planets*, in review, 1993b.

Betts, B. H., Edited Termoskan data files and descriptions, on the *PDS (Planetary Data System) Phobos '88 CD-ROM*, produced in May 1992.

Murray,B.C., M.K.Naraeva, A.S.Selivanov, B.H.Betts, T.Svitek, V.D.Kharlamov, A.V.Romanov, M.L.Santee, Y.M.Gektin, D.A.Fomin, D.A.Paige, A.S.Panfilov, D.Crisp, J.W.Head, S.L.Murchie, and T.Z.Martin, Preliminary Assessment of Termoskan Observations of Mars, *Planetary and Space Science*, Vol. **39**, No. 1/2, pp. 237-265, 1991.

Abstracts

Betts, B. H. and B. C. Murray, Thermal Studies of Martian Channels and Valleys Using Termoskan Data, *Lunar Planet. Sci., XXIV*, 103-104, 1993.

Betts, B. H. and B. C. Murray, Thermally Distinct Ejecta Blankets from Martian Craters, in *Workshop on the Martian Surface and Atmosphere Through Time (MSATT), LPI Tech. Report 92-02*, 19-20, 1992.

Betts,B.H. and B.C.Murray, Martian Fluidized Ejecta Blankets as Seen in the Phobos '88 Termoskan Data Set, *Lunar Planet. Sci., XXII*, 97-98, 1991.

Betts, B. H., T. Svitek, M. L. Santee, B. C. Murray, D. Crisp, D. A. Paige, M. Naraeva, and A. Selivanov, "Preliminary quantitative assessment and analysis of Phobos 88 Termoskan observations of Mars": *Lunar Planet. Sci., XXI*, 77-78, 1990a.

Betts, *et al.*, (same as above), in *Scientific Results of the NASA-Sponsered Study Project on Mars: Evolution of Volcanism, Tectonics, and Volatiles* (Solomon, S. C., V. L. Sharpton, and J. R. Zimbelman, eds.), LPI Tech Rpt. 90-06, Lunar and Planetary Institute, Houston, 79-80, 1990b.

Betts,B.H., T.Svitek, M.L.Santee, B.C.Murray, D.Crisp, D.A.Paige, M.Naraeva, and A.Selivanov, Preliminary Quantitative Assessment and Analyses of Phobos '88 Termoskan Observations of Mars, *Brown-Vernadsky Microsymposium*, 1990c.

Ksanfomality, L.V., V.I. Moroz, A.V. Zharkov, G.E. Nikitin, M.L. Santee, D. Crisp, T.Z. Martin, D.A. Paige, B.H. Betts, B.C. Murray, F.D. Palluconi, P. Bibring, M. Comb, and A. Soufflot, "Preliminary features of KRFM observations of Mars": published at International Symposium: First Results of the Phobos-Mars Mission and Future Space Exploration of Mars, in Paris, France, Oct. 1989.

Selivanov, A., M.K. Naraeva, V. Kharlomov, A. Romanov, Y.M. Gektin, D.A. Paige, B.H. Betts, and B.C. Murray, "Comparisons between infrared thermal emission measurements of Mars by Phobos Termoskan and Viking IRTM": published at International Symposium: First Results of the Phobos-Mars Mission and Future Space Exploration of Mars, in Paris, France, Oct. 1989.

ABSTRACT

Utilizing the Termoskan data set of the Phobos '88 mission we have recognized a new feature on Mars: Ejecta blanket Distinct In the THermal infrared (EDITH). Virtually all of the more than one hundred of these features discovered in the Termoskan data are located on the plains near Valles Marineris. EDITHs have a startlingly clear dependence upon terrains of Hesperian age, implying a spatial or temporal dependence on Hesperian terrains. Almost no thermally distinct ejecta blankets are associated with any of the thousands of craters within the data set that occur on the older Noachian units. EDITHs also do not appear on the portions of the younger Tharsis Amazonian units seen in the data. The Hesperian terrain dependence cannot be explained by either atmospheric or impactor variations; Noachian and Hesperian terrains must have experienced identical atmospheric and impactor conditions during Hesperian times. Thermally distinct ejecta blankets therefore reflect target material differences and/or secondary modification processes.

Not all lobate ejecta blankets are thermally distinct, but all EDITHs correlated with visibly discernible ejecta blankets are associated with lobate ejecta blankets. The boundaries of the thermally distinct areas usually follow closely the termini of the fluidized lobate ejecta blankets, even when the ejecta blankets show a high degree of sinuosity. Thus, the thermally distinct nature of EDITHs must be due to the primary ejecta formation process. The coupling of these thermal anomalies to morphology is unlike most sharp martian inertia variations which are decoupled from observed surface morphology. Some thermally distinct ejecta blankets occur near otherwise similar craters that do not have thermally distinct ejecta blankets. Thus, wind patterns or locally available aeolian material cannot provide a single overall explanation for the observed variations. We compiled a database of 110 EDITH and non-EDITH craters ranging in diameter from 4.2 km to 90.6 km. There are almost no correlations within the database other than occurrence on Hesperian terrains.

We postulate that most of the observed EDITHs are due to excavation of thermally distinctive Noachian age material from beneath a relatively thin layer of younger, more

consolidated Hesperian volcanic material. The plausibility of this theory is supported by much geological evidence for relatively thin near-surface Hesperian deposits overlying massive Noachian megabreccias on the EDITH-rich plains units. We suggest that absence of thermally distinct ejecta blankets on Noachian and Amazonian terrains is due to absences of distinctive near-surface layering. Thermally distinct ejecta blankets are excellent locations for future landers and remote sensing because of relatively dust free surface exposures of material excavated from depth.

ABSTRACT

The Termoskan instrument on board the Phobos '88 spacecraft acquired the highest spatial resolution thermal data ever obtained for Mars. Included in the thermal images are 2 km per pixel, midday observations of several major channel and valley systems including significant portions of Shalbatana Vallis, Ravi Vallis, Al-Qahira Vallis, Ma'adim Vallis, the channel connecting Valles Marineris with Hydraotes Chaos, and channel material, in Eos Chasma. Termoskan also observed small portions of the southern beginnings of Simud, Tiu, and Ares Valles and some channel material in Gangis Chasma. Simultaneous broad band visible data were obtained for all but Ma'adim Vallis. We find that most of the channels and valleys have higher inertias than their surroundings, consistent with previous thermal studies of martian channels. We show for the first time that thermal inertia boundaries closely match all flat channel floor boundaries. Lower bounds on typical channel thermal inertias range from 8.4 to 12.5 (10^{-3} cal cm^{-2} $s^{-1/2}$ K^{-1}). Lower bounds on inertia differences with the surrounding heavily cratered plains range from 1.1 to 3.5. Atmospheric and geometric effects are not sufficient to cause the inertia enhancements. We agree with previous researchers that localized, dark, high inertia areas within channels are likely aeolian in nature. However, our data show that aeolian deposits do not fill the channels, nor are they responsible for the overall thermal inertia enhancement. Thermal homogeneity and strong correlation of thermal boundaries with the channel floor boundaries lead us to favor non-aeolian overall explanations. Flat floors and steep scalloped walls are observed in most regions that show increased inertia. Therefore, we favor fretting processes over catastrophic flooding for explaining the inertia enhancements. Fretting may have emplaced more blocks on channel floors or caused increased bonding of fines due to increased availability of water. Alternatively, post-channel formation water that was preferentially present due to the low, flat fretted floors may have enhanced bonding of original fines or dust fallout.

PRELIMINARY QUANTITATIVE ASSESSMENT AND ANALYSES OF PHOBOS 88 TERMOSKAN OBSERVATIONS OF MARS; B. H. Betts, T. Svitek, M. L. Santee, B. C. Murray, D. Crisp, California Institute of Technology, D. A. Paige, University of California at Los Angeles, M. Naraeva and A. Selivanov, Institute of Space Devices, Moscow.

In February and March, 1989, the Termoskan instrument onboard the Phobos '88 spacecraft of the USSR acquired a limited set of very high resolution simultaneous observations of the reflected solar and thermal emission from Mars' equatorial region. We have analyzed quantitatively approximately 20% of the entire data set and here present three preliminary analyses: a comparison of Termoskan data with Viking Infrared Thermal Mapper (IRTM) data; an analysis of thermal infrared limb brightening seen on the morning limb and other preliminary limb analysis results; and an analysis of one observation of the shadow of the moon Phobos as observed on Mars by Termoskan.

THE EXPERIMENT: Termoskan was a two channel optical-mechanical scanning radiometer with one visible channel (0.5-1.0 μm and one thermal infrared channel (8.5-12.0 μm). The instrument was fixed to the spacecraft, pointing in the anti-solar direction. Resolution per pixel at nadir was 1.8 km for 3 of the 4 panoramas acquired and 300 meters for the remaining panorama.

COMPARISON WITH IRTM OBSERVATIONS: To determine the absolute accuracy of the Termoskan data set, we compared it with the well calibrated Viking IRTM measurements. We compared brightness temperatures from Termoskan infrared observations to brightness temperatures from IRTM's 11 micron channel (9.8 to 12.5 μm). We constrained the IRTM data to match approximately the Termoskan data in season (L_s), longitude, latitude, and local time of day. In order to compare the two data sets, we degraded the Termoskan resolution to a resolution comparable to Viking. Figure 1 shows a representative Termoskan-IRTM comparison which is consistent with other areas that we have compared. We find that the Termoskan brightness temperatures are approximately 3 K warmer than corresponding IRTM brightness temperatures; that relative features correlate very well in the two data sets; and that Termoskan sees thermal variations even at the limit of its spatial resolution.

TERMOSKAN LIMB PROFILES: Limb brightening in the Termoskan thermal infrared channel from the morning limb was consistently observed. Figure 2 shows a sample morning limb profile. We explain the peak in thermal brightness just off the limb as a consequence of an ice or dust haze in equilibrium with the atmosphere, which is warmer than the pre-dawn surface. Paige used a delta-Eddington spherical shell model developed for the Mars Observer limb sounder PMIRR (Pressure Modulator Infrared Radiometer), and found that a water ice haze with a scale height of 5 km (isothermal atmosphere at 200 K, surface at 175 K) could produce a thermal brightness signature matching the one in Figure 2. The visible channel defines a highly scattering atmosphere to extend 60 to 70 km above the limb. Figure 3 shows a sample evening limb profile. The absence of any infrared evening limb brightening is consistent with a surface which is warmer than the atmosphere . On the evening limb a high haze was observed which may correlate well with that seen by the Phobos '88 AUGUST experiment.

PHOBOS SHADOW MEASUREMENTS: Termoskan observed the shadow of Phobos on the surface of Mars during two of its four scans. Due to the scanning nature of the instrument and the similarity of the spacecraft's orbit to that of Phobos, the shadow appears elongated in the images. We have looked at one shadowed region south of Arsia Mons. We used the observed drop in visible flux within the shadowed area to model the solar insolation as a function of both actual time since the beginning of eclipse and position in the scan. We then used this in an adaptation of the Clifford et al., 1987 one dimensional, finite difference thermal model for a homogeneous surface [1]. By comparing the model results with the temperature drops observed in the infrared scan we find thermal inertias varying from 0.7 to 1.1 (10^{-3} cal cm^{-2} s$^{-1/2}$ K^{-1}). These values of thermal inertia are lower by factors of 2 to 4 compared to thermal inertias derived from Viking IRTM measurements [2] for the same area. Viking-derived inertias are sensitive to the upper few centimeters of the surface, whereas the Phobos shadow measurements are sensitive only to the upper tenths of a mm of the surface due to the short duration of the eclipse. Our results imply that there is a thin layer of highly insulating material, for example a thin, loosely packed dust layer, on the surface which overlies a layer of less insulating material.

REFERENCES: (1) Clifford, S.M., C.J. Bartels, and E.P. Rubenstein (1987), Lunar and Planetary Institute; (2) Kieffer, H.H., T.Z. Martin, A.P. Peterfreund, B.M. Jakosky, E.D. Miner, F.D. Palluconi (1977), Journal of Geophysical Research, 82 (28), pp. 4249-4291.

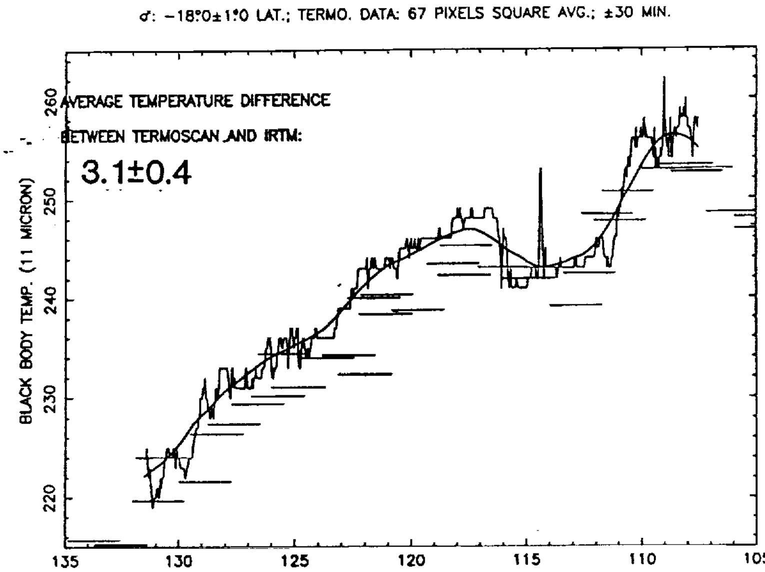

Figure 1: Comparison of Termoskan data with analogous IRTM data for a 2 degree wide strip of constant latitude centered on -18 degrees. The dark line represents a sliding boxcar average of Termoskan data which has been averaged in 2 x 2 degree squares. The lighter line is a 1 pixel Termoskan strip for reference. The points represent IRTM data with the error bars representing the footprint of each IRTM data point. IRTM data is constrained to match the Termoskan data to within ±10 degrees of L_s and to within ±30 minutes of local time. After comparing each IRTM point with the averaged Termoskan point of the same longitude, the average temperature difference between Termoskan and IRTM is 3.1±0.4 K with the Termoskan temperatures being warmer. Local time of day in the data shown ranges from about 8.5 to 10.3.

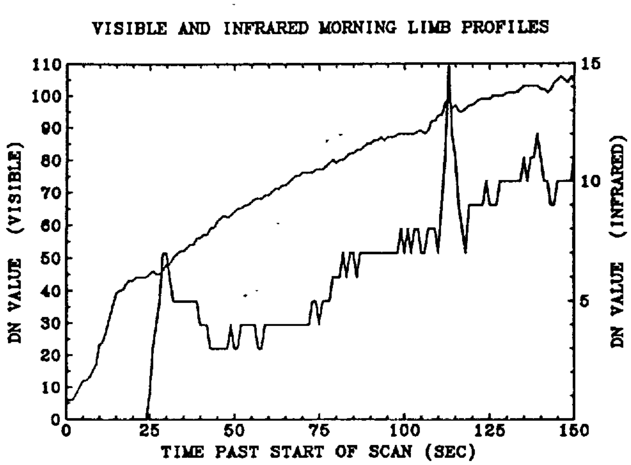

Figure 2: A single morning limb profile for both the visible (dashed curve) and the infrared (solid curve) channels. The solid limb was encountered at approximately 26 seconds after the start of the scan.

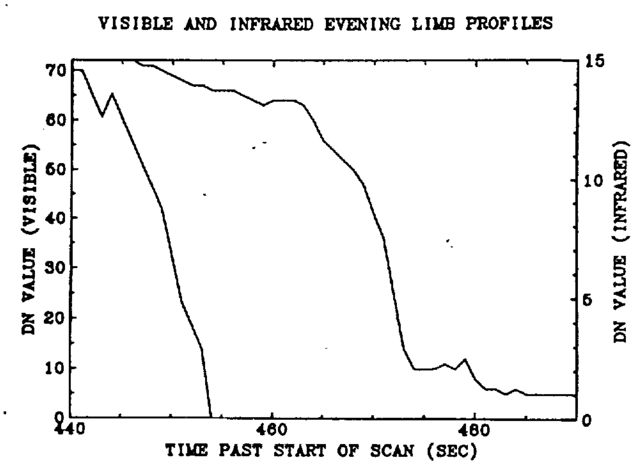

Figure 3: A single evening limb profile for both the visible (dashed curve) and the infrared (solid curve) channels. Note that the times on the horizontal axis are local to the particular data file and do not represent actual times along the scan. Note the peak in visible brightness at 479 seconds which is a distinct cloud feature.